PAPER

Performance Analysis of Fiber-Optic Relaying with Simultaneous Transmission and Reception on the Same Carrier Frequency

Hiroki UTATSU[†a)], ***Student Member and*** **Hiroyuki OTSUKA**[†b)], ***Senior Member***

SUMMARY Denser infrastructures can reduce terminal-to-infrastructure distance and thus improve the link budget in mobile communication systems. One such infrastructure, relaying can reduce the distance between the donor evolved node B (eNB) and user equipment (UE). However, conventional relaying suffers from geographical constraints, i.e., installation site, and difficulty in simultaneous transmission and reception on the same carrier frequency. Therefore, we propose a new type of fiber-optic relaying in which the antenna facing the eNB is geographically separated from the antenna facing the UE, and the two antennas are connected by an optical fiber. This structure aims to extend coverage to heavily shadowed areas. Our primary objective is to establish a design method for the proposed fiber-optic relaying in the presence of self-interference, which is the interference between the backhaul and access links, when the backhaul and access links simultaneously operate on the same carrier frequency. In this paper, we present the performance of the fiber-optic relaying in the presence of intra- and inter-cell interferences as well as self-interference. The theoretical desired-to-undesired-signal ratio for both uplink and downlink is investigated as parameters of the optical fiber length. We demonstrate the possibility of fiber-optic relaying with simultaneous transmission and reception on the same carrier frequency for the backhaul and access links. We validate the design method for the proposed fiber-optic relay system using these results.

key words: *mobile communication, relaying, fiber-optic technology, simultaneous transmission and reception, self-interference*

1. Introduction

Long term evolution (LTE) and LTE-Advanced mobile communication systems have been implemented worldwide as fourth-generation mobile systems. Currently, fifth-generation (5G) mobile systems are being developed, notably in the third-generation partnership project (3GPP). The primary objectives of 5G are to increase system capacity, improve data rates, improve cell-edge performance, achieve very low latency, and provide services based on Internet of Things [1]–[5].

From the network-density perspective, three approaches have been considered to increase system capacity and/or improve cell-edge performance.

The first approach is a fundamental small-cell strategy where a macro cell is divided into several small cells with smaller cell radius, i.e., the small-cell strategy reduces the coverage area of each cell and increases the total number of macro-cell sites [6], [7]. The specifications of each small cell are independent of one another. Each low-power evolved node B (eNB) in the small cell is directly connected to a core mobile network. Accordingly, this type of small cell is expected to improve system capacity compared with the traditional macro-only networks. In addition, the concept of a phantom cell has been proposed where small cells are overlaid on a macro cell [8]. This approach splits the control and user-data planes, i.e., the macro eNB manages all user equipment (UE) within the overlaid cells, although UE can connect to a neighboring low-power eNB in the small cell.

Heterogeneous network (HetNet) is an alternative approach for denser infrastructures. Pico cells with low-power eNBs are installed within the coverage area of a macro cell. The purpose of HetNet is to allow the UE to access the pico cells even though the UE is within the donor macro cell. HetNet can increase the system capacity, especially when the traffic in the macro cell enormously increases [9], [10].

Relaying is another technical approach that can be used to obtain dense infrastructures, in which the objective is to improve the cell-edge performance in a macro cell, i.e., to possibly realize UE high data rates. The relay node (RN) is installed around a macro-cell edge to recover, amplify and retransmit to the UE, a now strengthened but previously poor signal received from the donor eNB. Thus, relaying can physically reduce the distance between an eNB and UE [11]–[15]. In conventional relaying, the transmitter/receiver antennas facing the donor eNB and the different transmitter/receiver antennas facing UE are geographically located in the same place in a particular RN. However, the installation site of conventional RNs is also very limited, e.g., installing the conventional RN in heavily shadowed areas is difficult. Conventional relaying also suffers from a serious problem: if the carrier frequencies used for the backhaul (eNB–RN) and access (RN–UE) links are the same (i.e., inband relaying) and when the two links simultaneously operate, conventional relaying has difficulty avoiding self-interference between the transmitter and receiver antennas, or needs an interference canceller to eliminate the self-interference at the RN. When inband relaying is used, studies have suggested to avoid such interference in which the RN should separate the backhaul and access links with respect to time, i.e., time-division relaying [11]. On the other hand, when outband relaying is applied in which different carrier frequencies are used between two links, it can simultaneously transmit and receive because no self-interference is presented between the two links. However, this process

Manuscript received October 15, 2018.
Manuscript revised January 18, 2019.
Manuscript publicized February 20, 2019.
[†]The authors are with the the Graduate School of Engineering, Kogakuin University, Tokyo, 163-8677 Japan.
a) E-mail: cm18007@ns.kogakuin.ac.jp
b) E-mail: otsuka@cc.kogakuin.ac.jp
DOI: 10.1587/transcom.2018EBP3298

decreases the frequency-utilization efficiency. In [16]–[18], an interference canceller was proposed to eliminate the self-interference. However, the cost and stability for mobile systems would be considered.

Recently, full duplex (FD) schemes have been discussed for simultaneous transmission and reception on the same carrier frequency to increase frequency utilization efficiency, although frequency division duplex (FDD) or time division duplex (TDD) schemes have been used for mobile communication systems [19], [20]. In [19], self-interference cancellation has been discussed to eliminate the self-interference between downlink and uplink, in which self-interference canceller equipped with eNB can eliminate the self-interference (produced by the downlink signal to other UE) from desired uplink signal of a target UE. Like this, self-interference cancellation is one of key technology to establish FD mobile systems. However, in this paper, self-interference cancellation has not been concerned due to the same reason for RN with interference canceller.

On the basis of this background, we propose a new type of fiber-optic relaying in which the antenna facing the eNB is geographically separated from the antenna facing the UE, and the two antennas are connected by an optical fiber. The first purpose is to facilitate the installation of an RN. For example, the antenna facing the eNB can be installed where the received signal power from the eNB is very high, and the antenna facing UEs can be placed where the received signal power from the eNB is very low, i.e., in heavily shadowed areas. The second purpose is to realize simultaneous transmission and reception on the same carrier frequency between the backhaul (eNB–RN) and access (RN–UE) links [21]–[24].

In this work, we present an overview of the proposed fiber-optic relaying in comparison with conventional relaying technology and demonstrate the transmission performance of fiber-optic relaying under the conditions of simultaneous transmission and reception on the same carrier frequency considering the presence of self-, intra-cell, and inter-cell interferences. Specifically, the theoretical desired-to-undesired-signal ratio (DUR) is investigated for both uplink and downlink using a specific cell layout model as parameters of the optical fiber length.

The key contributions of this work can be summarized as follows.

- We propose a new type of fiber-optic relaying to facilitate the installation method and to enable simultaneous transmission and reception on the same carrier frequency between the backhaul (eNB–RN) and access (RN–UE) links.
- We clarify the DUR performance of the proposed fiber-optic relaying by considering the intra- and inter-cell interferences as well as self-interference for both uplink and downlink using a specific cell layout model as parameters of the optical fiber length.

This paper is organized as follows. In Sect. 2, we introduce the proposed fiber-optic relaying architecture. In Sect. 3, we provide the self-interference mechanism when inband relaying is used. In Sect. 4, we present the theoretical results such as the DUR using the specific cell layout model. Finally, we conclude our work in Sect. 5.

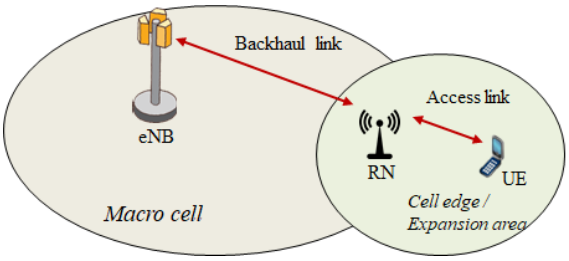

Fig. 1 Conventional relaying.

2. System Overview

Figure 1 shows a typical conventional relay system. The RN is introduced by wirelessly connecting it to the network via a donor eNB in the macro cell. Consequently, the UE located at the cell edge is connected to the eNB via the adjacent RN. Here the link between the donor eNB and RN is defined as the backhaul link (eNB–RN), and that between the RN and UE is called the access link (RN–UE).

Several types of relay systems have been envisioned, and some of these have already been established in the 3GPP standardization [11]. A basic requirement for relaying is that the relay should be transparent to the UE. A non-regenerative relay type, i.e., an amplify-and-forward relay is very simple and is commonly referred to as repeaters. The repeater principle is to amplify only the received signals, including the noise and interference as well as the desired signal, so that the RN should be installed at high signal-to-interference plus noise ratio (SINR) environments. This relay type does not have its own physical cell ID and does not transmit its common control signals. On the other hand, the regenerative relay type, i.e., decode-and-forward relay, decodes and re-encodes the received signal and forwards it to the related UE. Therefore, this type of RN can be installed at relatively low-SINR environments compared with the repeaters. The decode-and-forward-type RN can control its cell using its own identity by transmitting its physical cell ID and common control signals to the related UE. UE located at cell edge can be connected to the RN by hearing these cell ID and common control signals, even though the UE cannot hear the control signal from donor eNB [25].

2.1 Fiber-Optic Relaying

The proposed fiber-optic relaying is illustrated in Fig. 2. The antenna facing the donor eNB (RN_{eNB}) is geographically separated from the antenna facing the UE (RN_{UE}), and the two are connected by optical fiber cables. Here, RN_{eNB} includes a transmitter antenna for the uplink and a receiver antenna for the downlink. RN_{UE} includes a transmitter antenna for the downlink and a receiver antenna for the uplink.

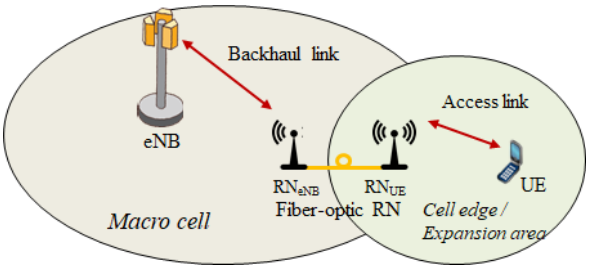

Fig. 2 Proposed fiber-optic relaying.

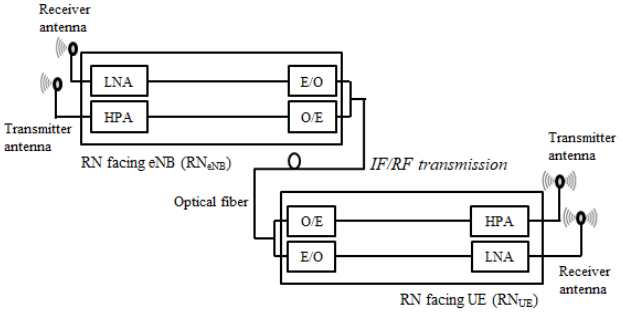

(a) Amplify-and-forward relay

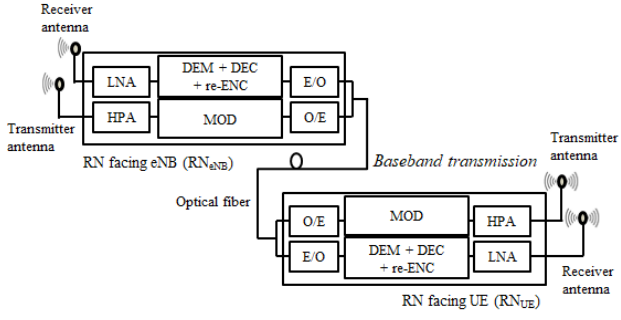

(b) Decode-and-forward relay

Fig. 3 Configuration of fiber-optic relaying.

Fiber-optic relaying can be applied to both amplify-and-forward and decode-and-forward relays, as shown in Fig. 3.

In the case of the amplify-and-forward relay, a modulated intermediate- or radio-frequency signal can be transmitted over the optical fiber, as shown in Fig. 3(a). The paired RN, i.e., RN_{eNB} and RN_{UE}, which contains a low-noise amplifier (LNA) and a high-power amplifier (HPA), is connected through an electric-to-optic converter (E/O), an optic-to-electric converter (O/E), and an optical fiber. By considering LTE as an example, orthogonal frequency division multiplexing (OFDM) signals directly modulate a laser diode (LD) or a distributed feedback LD within the E/O. At the O/E, a PIN-type photodiode (PD) or an avalanche PD converts the received optical signals into electrical signals with a linear response. In this case, the optical-link noise and nonlinearity should be evaluated, although the configuration is very simple.

In the case of the decode-and-forward relay, RN_{eNB} decodes and re-encodes the received signal from the eNB and forwards it to the related UE in the downlink. Figure 3(b) shows the block diagram example in which RN_{eNB} contains the LNA, demodulator (DEM), decoder (DEC), and re-encoder (re-ENC) for the downlink. RN_{UE} contains the modulator (MOD) and HPA for the downlink. Here, MOD and DEM include the up- and down-converter functions, respectively. In this case, the baseband signals are transmitted over the optical fiber, i.e., similar to digital transmission. Accordingly, the optical-link performance requirements are relaxed, and more economical E/O and O/E can be used compared with the case of the amplify-and-forward relay [26].

Usually, there are a few of transmission timing difference between eNB and RN_{UE} in the downlink, as well as conventional RN, because the fiber-optic RN has a transmission delay. To handle the transmission delay of fiber-optic RN as well as a propagation delay, UE can adjust the timing of its uplink transmission using a typical timing advance function [25], [27]. Therefore, the impact of RN delay is not highly critical in comparison with the delay of transport network, internet delay, and so on.

From the system cost perspective, fiber-optic relaying scheme may increase the system cost including the fiber-link installation cost compared to that of conventional relay system, however the fiber-optic relaying scheme is expected to provide higher performance for UEs, and also can facilitate the installation of RN in heavily shadowed areas.

In comparison with small cell deployment, fiber-optic relaying scheme is to improve the cell edge performance with wireless backhaul link, although it needs wired connection (optical fiber cables) between RN_{eNB} and RN_{UE}. On the other hand, small cell deployment needs wired connection between a network and the small cell sites, whose purpose is to increase system capacity. Like this, the purpose of fiber-optic relaying is different from that of small cell deployment. Mobile operator can choose better one to install according to the purpose.

2.2 Application Scenarios

Figure 4 shows the relaying system overview and application scenarios to extend the coverage to heavily shadowed areas. RN_{eNB} is located at the roof of a building, whereas the paired RN_{UE} is installed in heavily shadowed areas composed of obstacles and buildings [28]. In this case, the received SINR at RN_{eNB} is expected to be relatively high because the transmission link is fixed and the received antenna is located at a higher place. Therefore, fiber-optic relaying is expected to facilitate the introduction of a higher-order modulation scheme to increase the data rate. Until today, in the LTE systems, quadrature phase shift keying (QPSK), 16-quadrature amplitude modulation (QAM), and 64-QAM are being used for symbol modulation of OFDM. However, the use of fiber-optic relaying enables the application of higher-order modulation such as 256-QAM, 1024-QAM, and so on to the backhaul link between the eNB and RN_{eNB}. Conse-

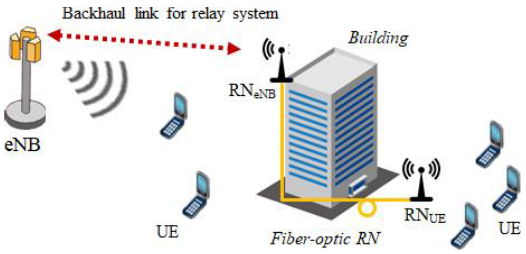

Fig. 4 System overview and application scenario.

quently, the throughput of the UE connected to RN_{UE} can be increased.

3. Analysis Model

As mentioned in the Introduction, from the carrier frequency perspective, relaying is classified into inband and outband relaying. Inband relaying uses the same carrier frequency between two links, i.e., backhaul and access links. On the other hand, outband relaying uses different carrier frequencies between two links.

3.1 Simultaneous Transmission and Reception on the Same Carrier Frequency

If inband relaying is used, the transmitter and receiver antennas must be isolated to prevent interference between the backhaul and access links. Time-division relay is mainly considered to avoid such interference between the backhaul and access links in which a conventional RN separates the backhaul and access links in terms of time, as shown in Fig. 5(a).

This process provides communication in both directions but not simultaneously. Figure 5(a) shows that when the eNB transmits data to the RN in the downlink, the RN cannot simultaneously relay the data to the UE. Specifically, the RN transmits only to the control channel without data, which is called as an almost blank subframe (ABS) [11], [29]. However, in this paper, we discuss inband relaying with simultaneous transmission and reception to further increase the frequency utilization efficiency. An example of subframe configuration is shown in Fig. 5(b) for fiber-optic relaying using the same carrier frequency, namely, f_1 or f_2, in which the radio frame and subframe are 10 ms and 1 ms, respectively. This process provides simultaneous communication in both directions and on the same carrier frequency.

3.2 Self-Interference

When the two (backhaul and access) links use the same carrier frequency simultaneously, the transmission in the access link interferes with the reception in the backhaul link in the downlink, as shown in Fig. 6(a) [18], [30]. The transmitted signal with power P_{RN} (transmission in the access link) causes interference U_{self} with the received desired-signal that originates from the eNB at RN_{eNB} (reception in the backhaul link). Generally, this type of interference is called "self-interference." At the receiver antenna of RN_{eNB}, both the desired signal with power P_r and undesired self-

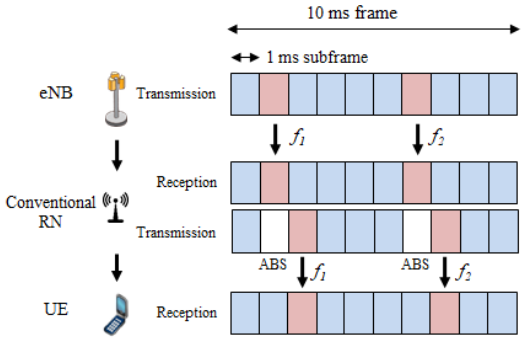

(a) Time-division relaying

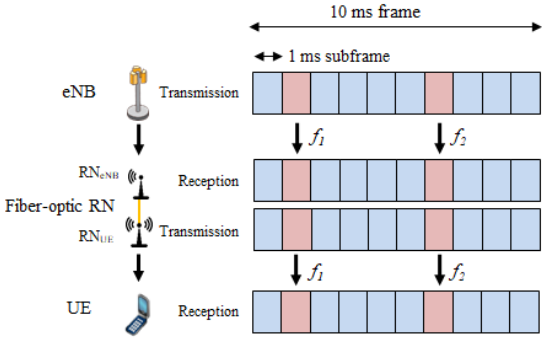

(b) Simultaneous relay on the same carrier frequency

Fig. 5 Configuration of the radio frame for fiber-optic relaying.

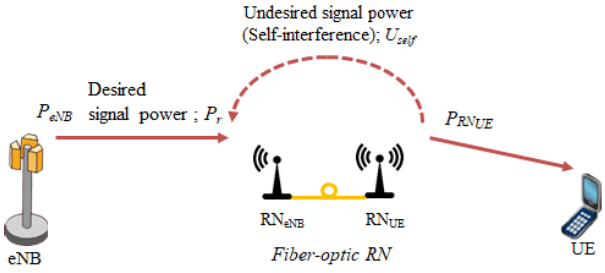

(a) In downlink

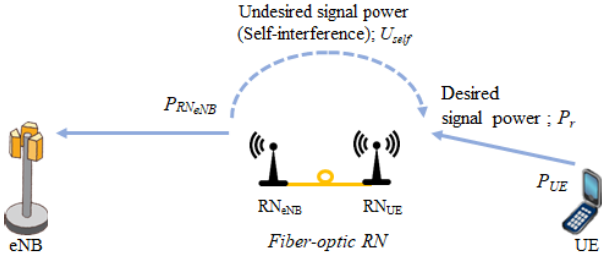

(b) In uplink

Fig. 6 Self-interference mechanism.

interference signal with power U_{self} are received. In this case, the DUR is defined as the ratio between P_r and U_{self}.

The uplink condition is also similar. The transmission in the backhaul link interferes with the reception in the access link, as shown in Fig. 6(b). The transmitted signal (transmission in the backhaul link) causes interference U_{self} with the received desired-signal that originates from the UE at $\mathrm{RN_{UE}}$ (reception in the access link). At the receiver antenna of $\mathrm{RN_{UE}}$, both the desired signal with power P_r and undesired self-interference signal with power U_{self} are simultaneously received.

As mentioned in 3.1, time-division relaying with ABS is superior compared to fiber-optic relaying in terms of DUR performance because of no self-interference.

3.3 Inter- and Intra-Cell Interferences

Frequency reuse is an important process in cellular mobile networks, and the frequency reuse factor of LTE is almost one, which inherently means that interference occurs among the different neighboring cells, especially at the cell edge, which is called inter-cell interference. UE receives interference from the neighboring cell, in addition to the desired signal from its server cell, when the same resource is simultaneously used. In addition, the UE creates interference on the neighboring cell in the uplink.

In this study, we consider the presence of such inter-cell interference, although the inter-cell interference coordination (ICIC) technology is widely used in radio resource management to mitigate the interference.

Similar to the inter-cell interference mechanism, interference is caused among different sectors in a macro cell, which is called intra-cell interference.

In this study, we use the cell layout model with seven cells and three sectors per cell, as shown in Fig. 7. Here, a single fiber-optic RN is located in the target sector, and single UE and a single conventional RN are located in each sector as interference sources for simplicity.

On the basis of these assumptions, total amount of interference U at the $\mathrm{RN_{eNB}}$ receiver in the downlink can be expressed as follows:

$$U = U_{self} + \sum_{i=1}^{2} \left(U_{intra,eNB(i)} + U_{intra,RN(i)}\right) + \sum_{j=1}^{6}\sum_{k=1}^{3} \left(U_{inter,eNB(j,k)} + U_{inter,RN(j,k)}\right) \quad (1)$$

where, $U_{intra,eNB(i)}$ is the intra-cell interference from $\mathrm{eNB_i}$ in the different sectors in the same macro cell, and $U_{intra,RN(i)}$ is the intra-cell interference from $\mathrm{RN_i}$ in the different sectors. Here, i denotes the sector identity number ($i = 1, 2$). $U_{inter,eNB(j,k)}$ is the inter-cell interference from neighboring $\mathrm{eNB_{i,k}}$, and $U_{inter,RN(j,k)}$ is the inter-cell interference from neighboring $\mathrm{RN_{j,k}}$. Here, j and k are the numbers of the cell and sector identities, respectively ($j = 1$ to 6, and $k = 1$ to 3). We assume that this interference is simultaneously received at $\mathrm{RN_{eNB}}$ in the downlink case.

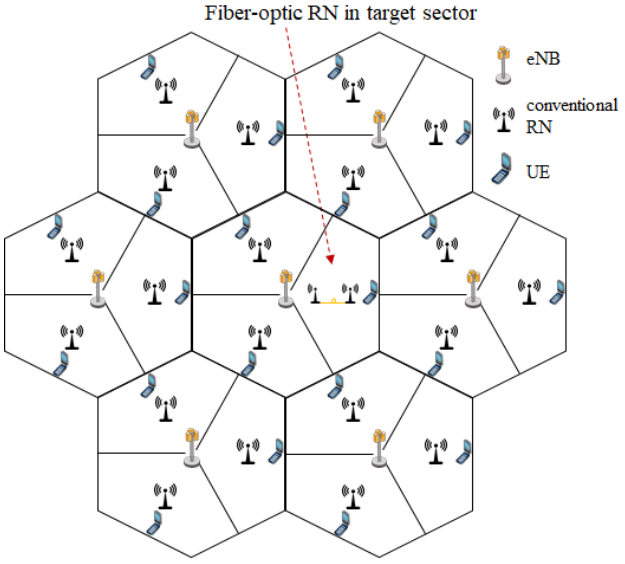

Fig. 7 Cell layout model with seven cells and three sectors per cell.

Similarly, the total amount of interference at the $\mathrm{RN_{UE}}$ receiver in the uplink can be expressed as follows:

$$U = U_{self} + \sum_{i=1}^{2} \left(U_{intra,UE(i)} + U_{intra,RN(i)}\right) + \sum_{j=1}^{6}\sum_{k=1}^{3} \left(U_{inter,UE(j,k)} + U_{inter,RN(j,k)}\right) \quad (2)$$

where, $U_{intra,UE(i)}$ is the intra-cell interference from the UE in the different sectors in the same macro cell, and $U_{intra,RN(i)}$ is the intra-cell interference from $\mathrm{RN_i}$ in the different sectors ($i = 1, 2$). $U_{inter,UE(j,k)}$ is the inter-cell interference from the UE located at neighboring $\mathrm{eNB_{i,k}}$. We also assume that this interference is simultaneously received at $\mathrm{RN_{UE}}$ in the uplink.

3.4 Path Loss Scenarios and Models

In this research, we use the ITU-R M.2135 model to calculate path loss in which three types of propagation scenarios are considered, namely, urban macro (UMa), urban micro (UMi), and indoor scenarios in dense urban environments [31]. We utilize different path-loss scenarios depending on the situation, as listed in Table 1. The propagation path between the eNB and $\mathrm{RN_{eNB}}$ uses the UMa scenario as well as the intra- and inter-cell interferences paths. The propagation path between $\mathrm{RN_{eNB}}$ and $\mathrm{RN_{UE}}$, i.e., self-interference path, uses the UMi scenario because the path distance is not so long. The propagation path between $\mathrm{RN_{UE}}$ and the related UE also uses the UMi scenario because the path distance is short and the antenna height of $\mathrm{RN_{UE}}$ is not very high.

Two types of path-loss models are defined. One is the path loss for line-of-sight (LOS), which is expressed as PL_{LOS}. Another is the path loss for non-line-of-sight

Table 1 Path Loss Scenario and Models used in Analysis.

Propagation path	Scenario	Path loss model
eNB – RN_{eNB}	UMa	PL_{LOS}, PL_{NLOS}
RN_{UE} – UE	UMi	PL_{LOS}, PL_{NLOS}
Self-interference	UMi	PL_{NLOS}
Inter-cell interference	UMa	PL_{NLOS}
Intra-cell interference	UMa	PL_{NLOS}

(NLOS), which is expressed as PL_{NLOS}. The PL_{LOS} and PL_{NLOS} for UMa are expressed in (3) and (4), respectively:

$$PL_{LOS} = 22\log_{10} d + 28 + 20\log_{10} f \tag{3}$$

$$\begin{aligned} PL_{NLOS} = {} & 161.04 - 7.1\log_{10} W + 7.5\log_{10} h \\ & - \left(24.37 - 3.7\,(h/h_1)^2\right)\log_{10} h_1 \\ & + (43.42 - 3.1\log_{10} h_1) \times (\log_{10} d - 3) \\ & + 20\log_{10} f - \left(3.2\,(\log_{10}(11.75h_2))^2 - 4.97\right) \end{aligned} \tag{4}$$

where, f (Hz) is the carrier frequency, and h_1 and h_2 (m) are the heights of the transmitter and receiver antennas, respectively. h is the average building height, and W (m) is the street width. d (m) is the distance between the transmitter and receiver antennas. For the case of the self-interference path, d denotes the horizontal distance between RN_{eNB} and RN_{UE}, which is assumed to be equal to the optical fiber length.

The PL_{LOS} for UMi is common for UMa as defined in (3). The PL_{NLOS} for UMi is specified as:

$$PL_{NLOS} = 36.7\log_{10} d + 22.7 + 26.0\log_{10} f \tag{5}$$

Two types of path loss models, PL_{LOS} or PL_{NLOS}, are used for the propagation path between eNB and RN_{eNB}, and the propagation path between RN_{UE} and UE. Self-interference path uses only PL_{NLOS}, because the path provides severe condition although the distance is not so long. The propagation path for both inter-cell and intra-cell interference also uses PL_{NLOS}.

4. Numerical Results

4.1 Analysis Conditions

The primary parameters used in the analysis are listed in Table 2. The carrier frequency is 2 GHz. The transmission power of eNB, RN_{UE}, and UE are 46, 30, and 23 dBm, respectively. The uplink transmission power of conventional RN and RN_{eNB} are assumed to be 23, 26, and 30 dBm. Three sectors per cell are assumed, namely three sector antennas at each eNB are used. Figure 8 shows the details of Fig. 7 used in the simulation. RN_{eNB} is installed at a distance of 100 or 150 m away from the eNB on the center line of the target sector, as shown in Fig. 8(a). Similarly, UE is located at a distance of 250 m away from the eNB. In Fig. 7, the distance between eNBs next to each other is fixed to 500 m. Conventional RNs are installed as interference sources in each sector except the target sector as shown in Fig. 7. The

Table 2 Primary Parameters used in the Analysis.

Parameter	Value
Carrier frequency	2.0 GHz
eNB transmission power, P_{eNB}	46 dBm
eNB transmitter/receiver antenna height	25 m
eNB transmitter antenna gain	17 dBi
RN_{eNB} transmission power, P_{RNeNB}	23/26/30 dBm
RN_{UE} transmission power, P_{RNUE}	30 dBm
RN_{eNB} transmitter/receiver antenna height	10 m
RN_{eNB} receiver antenna gain	7 dBi
RN_{UE} transmitter/receiver antenna height	5 m
RN_{UE} receiver antenna gain	5 dBi
Conventional RN downlink transmission power	30 dBm
Conventional RN uplink transmission power, P_{RN}	23/26/30 dBm
UE transmission power, P_{UE}	23 dBm
UE transmitter/receiver antenna height	1.5 m
UE transmitter antenna gain	0 dBi
Distance between eNBs	500 m
Distance between eNB and RN_{eNB}	100, 150 m
Distance between eNB and conventional RN	175 m
Distance between eNB and UE	250 m

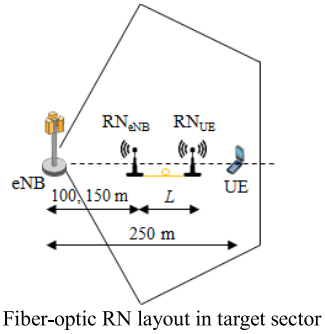

(a) Fiber-optic RN layout in target sector

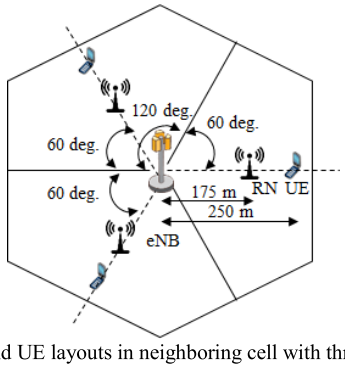

(b) RN and UE layouts in neighboring cell with three sectors

Fig. 8 Layout models used in the analysis.

conventional RN is installed at a distance of 175 m away from the eNB on the center line of each sector, as shown in Fig. 8(b). UE is located at a distance of 250 m away from the eNB in each sector.

eNB sector antenna pattern is referred to in [31]. RN_{eNB} antenna pattern is referred to in [32]. As shown in [31], horizontal antenna pattern used for eNB sector antenna is specified as:

$$A_h(\theta) = -min\left[12\left(\frac{\theta}{\theta_{3dB}}\right)^2,\ A_m\right] \tag{6}$$

where $A_h(\theta)$ is the relative antenna gain in the direction

θ, A_m is the maximum attenuation, and θ_{3dB} is the 3 dB beamwidth. The vertical antenna pattern is given by:

$$A_v(\phi) = -min\left[12\left(\frac{\phi - \phi_{tilt}}{\phi_{3dB}}\right)^2,\ SLA_v\right] \tag{7}$$

where $A_v(\phi)$ is the relative antenna gain in the vertical direction ϕ, SLA_v is the maximum attenuation, ϕ_{tilt} is the tilt angle. The combined antenna pattern is calculated as:

$$A(\theta, \phi) = -min\left[-(A_h(\theta) + A_v(\varphi)),\ A_m\right] \tag{8}$$

where $A(\theta, \phi)$ is the relative total antenna gain.

$\mathrm{RN_{eNB}}$ antenna pattern is almost similarly configured.

4.2 DUR Performance

Downlink DUR is defined as the ratio of received desired-signal power P_r at the $\mathrm{RN_{eNB}}$ receiver antenna as shown in Fig. 6(a), and total amount of interference U defined in (1). In the analysis, we assume that the intra-cell interference from the $\mathrm{eNB_i}$ in the different sectors in the same macro cell, namely, $U_{intra,eNB(i)}$, is completely suppressed because of the limitation in the sector antenna radiation patterns. The uplink DUR can be similarly obtained using received desired-signal power P_r at the $\mathrm{RN_{UE}}$ receiver antenna, as shown in Fig. 6(b) and total amount of interference U defined in (2).

In this study, we obtain both downlink and uplink DURs as the parameters of L for the distances between eNB and $\mathrm{RN_{eNB}}$ of 100 and 150 m, respectively. We also analysis downlink DUR under the conditions of both PL_{LOS} and PL_{NLOS} for the propagation path between eNB and $\mathrm{RN_{eNB}}$. In this case, the DUR when PL_{LOS} is used for the propagation path between $\mathrm{RN_{UE}}$ and UE is same as that when PL_{NLOS} is used, because the path has no impact for the DUR. Likewise, we analysis uplink DUR under the conditions of both PL_{LOS} and PL_{NLOS} for the propagation path between $\mathrm{RN_{UE}}$ and UE. In this case, the DUR when PL_{LOS} is used for the propagation path between eNB and $\mathrm{RN_{eNB}}$ is same as that when PL_{NLOS} is used, because the path has no impact for the DUR.

Figures 9 to 12 shows the downlink DUR performance, on the other hand, the uplink DUR performance are provided in Figs. 13 to 16. In these figures, we refer to DUR defined by total amount interference as D/U, and DUR defined by only self-interference as $\mathrm{D/U_{self}}$.

Figures 9 and 10 show the downlink DUR versus L when the distance between eNB and $\mathrm{RN_{eNB}}$ is 100 m. The difference is, Fig. 9 is the DUR when PL_{LOS} is used for the propagation path between eNB and $\mathrm{RN_{eNB}}$, while Fig. 10 is the DUR when PL_{NLOS} is used. Figure 9 shows that the downlink DUR is fixed in the range greater than $L = 40$ m because the inter-cell interference is observed to be dominant, however, U_{self} decreases according to the increase in L. When L is shorter than approximately 40 m, self-interference U_{self} is dominant. Assuming that the DUR benchmark is 30 dB, the downlink DUR can satisfy the benchmark in the range greater than $L = 10$ m. When

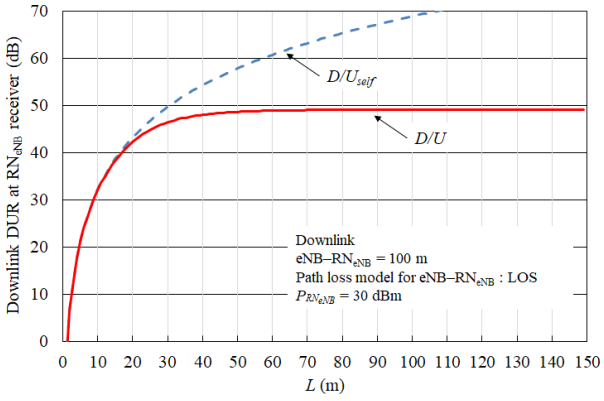

Fig. 9 Downlink DUR when the distance between eNB and $\mathrm{RN_{eNB}}$ is 100 m and path loss model for eNB – $\mathrm{RN_{eNB}}$ is LOS.

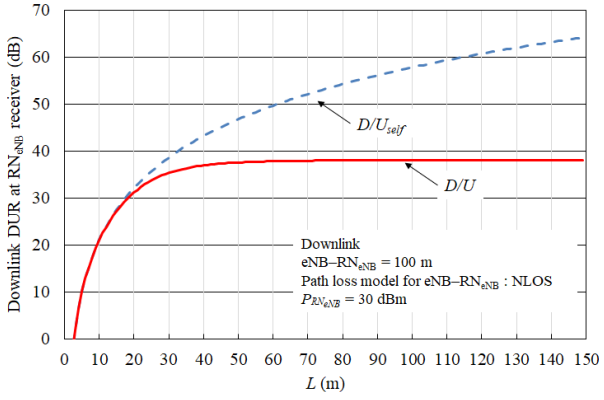

Fig. 10 Downlink DUR when the distance between eNB and $\mathrm{RN_{eNB}}$ is 100 m and path loss model for eNB – $\mathrm{RN_{eNB}}$ is NLOS.

PL_{NLOS} is used for the propagation path between eNB and $\mathrm{RN_{eNB}}$, the downlink DUR worsens because received desired-signal power decreases. In this case, the downlink DUR can satisfy the benchmark in the range greater than $L = 20$ m.

Figures 11 and 12 show the downlink DUR when the distance between eNB and $\mathrm{RN_{eNB}}$ is 150 m. Figure 11 is the downlink DUR when PL_{LOS} is used for the propagation path between eNB and $\mathrm{RN_{eNB}}$, while Fig. 12 is the downlink DUR when PL_{NLOS} is used. The behavior observed is similar to that shown in Figs. 9 and 10. Compared with the case of the eNB–$\mathrm{RN_{eNB}}$ distance of 100 m, the downlink DUR worsens because received desired-signal power decreases, although the self-interference is the same as that for the eNB–$\mathrm{RN_{eNB}}$ distance of 100 m. The downlink DUR can meet the benchmark of 30 dB in the range greater than L of approximately 20 m as shown in Fig. 11. However, when PL_{NLOS} is used, the downlink DUR can no longer meet the benchmark.

Figures 13 and 14 show the uplink DUR versus L when the distance between eNB and $\mathrm{RN_{eNB}}$ is 100 m. Figure 13 is the uplink DUR when PL_{LOS} is used for the propagation path between $\mathrm{RN_{UE}}$ and UE, while Fig. 14 is the uplink DUR when PL_{NLOS} is used. The intra- and inter-cell

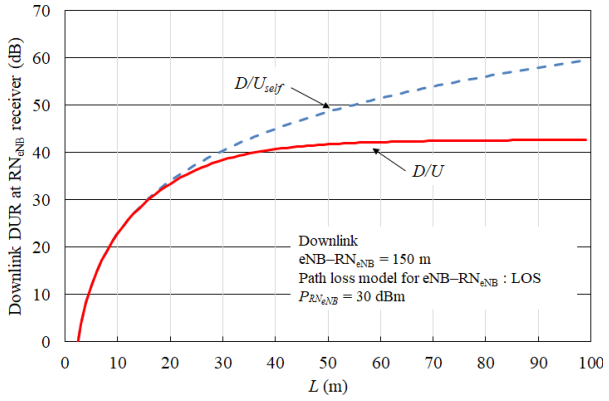

Fig. 11 Downlink DUR when the distance between eNB and RN$_{eNB}$ is 150 m and path loss model for eNB – RN$_{eNB}$ is LOS.

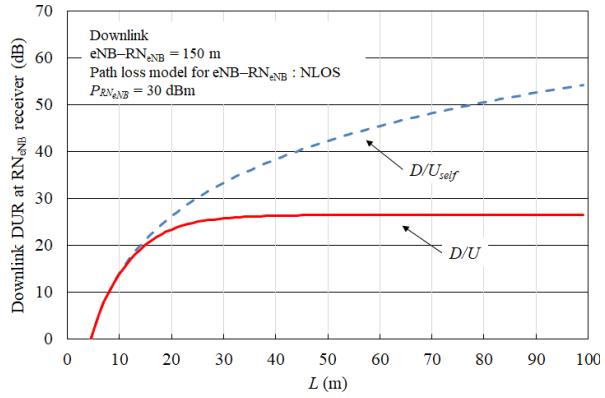

Fig. 12 Downlink DUR when the distance between eNB and RN$_{eNB}$ is 150 m and path loss model for eNB – RN$_{eNB}$ is NLOS.

interferences are observed to be much greater than the self-interference. Therefore, the minimum L required to satisfy the DUR benchmark depends on the intra- and inter-cell interference, and L = 136 m can meet a DUR of 30 dB, as shown in Fig. 13. When PL_{NLOS} is used for the propagation path between RN$_{UE}$ and UE, the uplink DUR worsens because received desired-signal power decreases. In this case, the downlink DUR can satisfy the benchmark in the range greater than L = 142 m.

Figures 15 and 16 show the uplink DUR when the distance between eNB and RN$_{eNB}$ is 150 m. Figure 15 is the uplink DUR when PL_{LOS} is used for the propagation path between RN$_{UE}$ and UE, while Fig. 16 is the uplink DUR when PL_{NLOS} is used. The behavior observed is similar to that shown in Figs. 13 and 14. Compared with the case of the eNB–RN$_{eNB}$ distance of 100 m, the uplink DUR is improved because received desired-signal power increases, although the self-interference is the same as that for the eNB–RN$_{eNB}$ distance of 100 m. For example, the uplink DUR can meet the benchmark of 30 dB in the range greater than L of approximately 82 m as shown in Fig. 15.

Thus, the minimum L that satisfies the DUR benchmark depends on the uplink performance. However, if the ICIC technology is applied, especially in the uplink, to mitigate the interference under the radio resource management, the minimum L needed to meet the DUR benchmark will decrease, or depend on the downlink DUR performance.

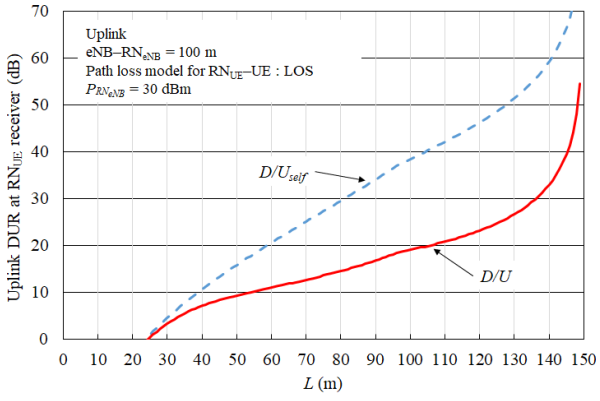

Fig. 13 Uplink DUR when the distance between eNB and RN$_{eNB}$ is 100 m and path loss model for RN$_{UE}$ – UE is LOS.

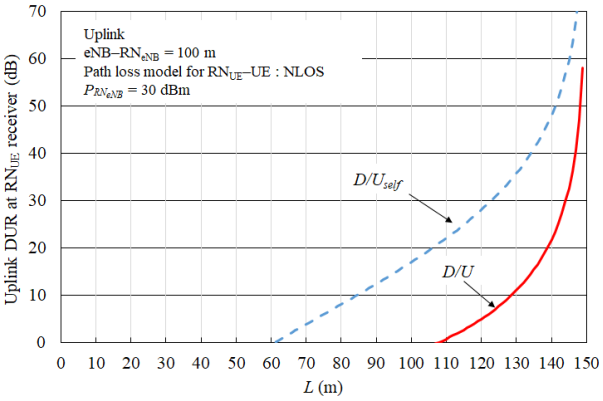

Fig. 14 Uplink DUR when the distance between eNB and RN$_{eNB}$ is 100 m and path loss model for RN$_{UE}$ – UE is NLOS.

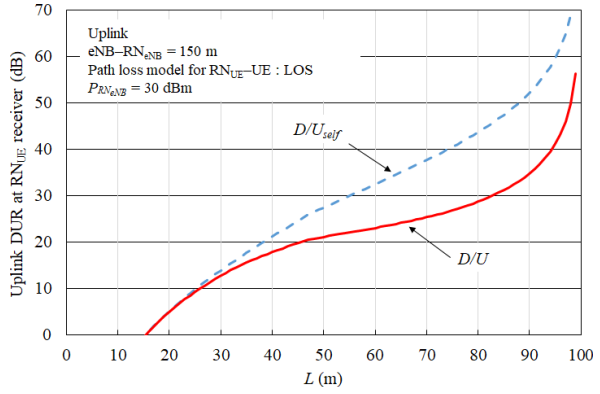

Fig. 15 Uplink DUR when the distance between eNB and RN$_{eNB}$ is 150 m and path loss model for RN$_{UE}$ – UE is LOS.

Figure 17 shows the uplink DUR versus L when the distance between eNB and RN$_{eNB}$ is 100 m, and PL_{LOS} is used for the propagation path between RN$_{UE}$ and UE, as parameters of the uplink transmission power of conventional RN and RN$_{eNB}$, i.e., P_{RN} and P_{RNUE}, respectively. When the

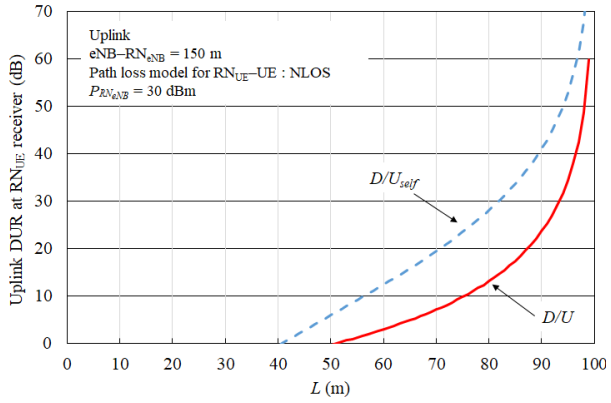

Fig. 16 Uplink DUR when the distance between eNB and RN_{eNB} is 150 m and path loss model for RN_{UE} – UE is NLOS.

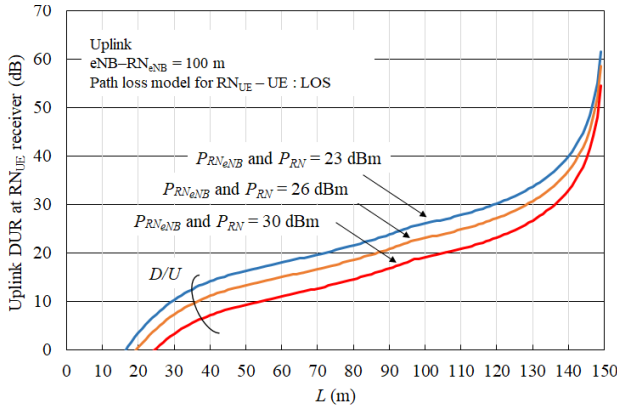

Fig. 17 Uplink DUR versus L as parameters of the transmission power of RN_{eNB} and RN.

uplink transmission power P_{RN} and P_{RNUE} are 23 dBm, the uplink DUR can satisfy the benchmark in the range greater than L = 120 m. That is, the minimum L required to satisfy the DUR benchmark for P_{RN} and P_{RNUE} of 23 dBm can be improved by 16 m in comparison with those transmission power of 30 dBm. Consequently, the transmission power P_{RN} and P_{RNUE} should be lower on the condition that the uplink signals from the RN_{eNB} and RN are demodulated normally at each eNB receiver.

5. Conclusion

In this paper, we have proposed a new type of fiber-optic relaying in which the antenna facing the eNB (RN_{eNB}) is geographically separated from the antenna facing the UE (RN_{UE}), and the two antennas are connected by an optical fiber. First, we have described the overview and benefits of fiber-optic relaying with simultaneous transmission and reception when the same carrier frequency is used between the backhaul and access links. Then, we have presented the theoretical DUR performance of the fiber-optic relaying under intra- and inter-cell interferences as well as the self-interference using a practical cell layout in both downlink and uplink.

Numerical analyses have clarified both the downlink and uplink DURs as parameters of optical fiber length L, which is equal to the horizontal distance between RN_{eNB} and RN_{UE}, provided that the carrier frequency is 2 GHz. We have confirmed that the minimum L required to satisfy the DUR benchmark is determined by the uplink DUR, and a longer distance between eNB and RN_{eNB} worsens the downlink DUR and improves the uplink DUR. Assuming that the DUR benchmark is 30 dB, the downlink DUR can satisfy the benchmark in the range greater than L = 10 m, when the distance between eNB and RN_{eNB} is 100 m, and PL_{LOS} is used for the propagation path between eNB and RN_{eNB}. Under the same distance condition, the uplink DUR can satisfy the benchmark in the range greater than L = 120 m, when the uplink transmission power of conventional RN and RN_{eNB} are 23 dBm, and PL_{LOS} is used for the propagation path between RN_{UE} and UE.

In our future work, we will clarify user throughput performance of the fiber-optic relaying under the conditions of multiple cell layout using system-level computer simulation, and also make a comparison between fiber-optic relaying and time-division relaying with ABS.

Acknowledgments

This work was supported in part by JSPS KAKENHI Grant Number JP18K11277, Grant-in-Aid for Scientific Research (C). This work was also supported in part by NTT DOCOMO, INC.

References

[1] 3GPP TR 36.912 version 11, "Feasibility study for further advancements for E-UTRA (LTE-Advanced)," Sept. 2012.
[2] 3GPP News, "3GPP system standards heading into the 5G era," http://www.3gpp.org/news-events/3gpp-news/1614-sa_5g, 2014.
[3] J.G. Andrews, S. Buzzi, W. Choi, S.V. Hanly, A. Lozano, A.C.K. Soong, and J.C. Zhang, "What will 5G be?," IEEE J. Sel Areas Commun., vol.32, no.6, pp.1065–1082, June 2014.
[4] D. Soldani and A. Manzalini, "Horizon 2020 and beyond; On the 5G operating system for a truly digital society," IEEE Veh. Technol. Mag., vol.10, no.1, pp.32–42, March 2015.
[5] Z. Gao, L. Dai, D. Mi, Z. Wang, M.A. Imran, and M.Z. Shakir, "MmWave massive-MIMO-based wireless backhaul for the 5G ultra-dense network," IEEE Wireless Commun., vol.22, no.5, pp.13–21, Oct. 2015.
[6] E. Dahlman, K. Dimou, S. Parkvall, and H. Tullberg, "Future wireless access small cells and heterogeneous deployments," Proc. ICT 2013, May 2013.
[7] A.R. Elsherif, W.P. Chen, A. Ito, and Z. Ding, "Resource allocation and inter-cell interference management for dual-access small cells," IEEE J. Sel. Areas Commun., vol.33, no.6, pp.1082–1096, March 2015.
[8] H. Ishii, Y. Kishiyama, and H. Takahashi, "A novel architecture for LTE-B: C-plane/U-plane split and phantom cell concept," Proc. Globecom Workshop, pp.624–630, Dec. 2012.
[9] A. Ghosh, R. Ratasuk, B. Mondai, N. Mangalvedhe, and T. Thomas, "LTE-advanced: Next-generation wireless broadband technology," IEEE Wireless Commun., vol.17, no.3, pp.10–22, June 2010.
[10] Qualcomm, "LTE Advanced: Heterogeneous Networks," Qualcomm HP, Jan. 2011.

[11] 3GPP TR 36.806 (V9.0.0), "Relay architectures for E-UTRA (LTE-Advanced)," March 2010.
[12] A.B. Saleh, S. Redana, B. Raaf, T. Riihonen, J. Hamalainen, and R. Wiehman, "Performance of amplify-and-forward and decode-and-forward relays in LTE-advanced," Proc. VTC2009-Fall, Sept. 2009.
[13] O. Bulakci, S. Redana, B. Raaf, and J. Hamalainen, "Performance enhancement in LTE-advanced relay networks via relay site planning," Proc. VTC2010-Spring, May 2010.
[14] Y. Bo, L. Yang, X. Cheng, and R. Cao, "Transmit power optimization for full duplex decode-and-forward relaying," Proc. Globecom 2013, pp.3347–3352, Dec. 2013.
[15] A. Sabharwal, P. Schniter, D. Guo, D.W. Bliss, S. Rangarajan, and R. Wichman, "In-band full-duplex wireless: Challenges and opportunities," IEEE J. Sel. Areas Commun., vol.32, no.9, pp.1637–1652, Sept. 2014.
[16] R. Lopez-Valcarce, E. Antonio-Rodriguez, C. Mosquera, and F. Perez-Gonzalez, "An adaptive feedback canceller for full-duplex relays based on spectrum shaping," IEEE J. Sel. Areas Commun., vol.30, no.8, pp.1566–1577, Aug. 2012.
[17] K. Hayashi, Y. Fujishima, M. Kaneko, H. Sakai, R. Kudo, and T. Murakami, "Self-interference canceller for full-duplex radio relay station using virtual coupling wave paths," Proc. APSIPA ASC 2012, Dec. 2012.
[18] Z. Zhang, X. Chai, K. Long, A.V. Vasilakos, and L. Hanzo, "Full duplex techniques for 5G networks: self-interference cancellation, protocol design, and relay selection," IEEE Commun. Mag., vol.53, no.5, pp.128–137, May 2015.
[19] J.I. Choi, M. Jain, K. Srinivasan, P. Levis, and S. Katti, "Achieving single channel, full duplex wireless communication," Proc. MobiCom2010, pp.1–12, Sept. 2010.
[20] K. Yamazaki, Y. Sugiyama, Y. Kawahara, S. Saruwatari, and T. Watanabe, "Preliminary evaluation of simultaneous data and power transmission in the same frequency channels," Proc. WCNC2015, pp.1237–1242, March 2015.
[21] H. Otsuka, N. Tanoi, and A. Nakajima, "Performance analysis of fiber-optic relaying in the presence of interferences between backhaul and access links," Proc. VTC2013-Fall, 8D-6, Sept. 2013.
[22] H. Otsuka, N. Tanoi, N. Ogura, T. Kubo, T. Asai, and Y. Okumura, "Performance analysis of fiber-optic inband relaying in the presence of self-interferences," Proc. VTC2014-Fall, 9H-3, Sept. 2014.
[23] S. Nakazawa, K. Iwai, M. Nakamura, T. Kubo, T. Asai, Y. Okumura, and H. Otsuka, "Performance of fiber-optic inband relaying against self-interference in both uplink and downlink," Proc. VTC2015-Fall, 9D-4, Sept. 2015.
[24] R. Nakao, N. Naganuma, S Takano, and H. Otsuka, "Performance analysis of fiber-optic inband relaying against both self- and inter-cell interference," Proc. VTC2017-Fall, 8P-9, Sept. 2017.
[25] M. Iwamura, H. Takahashi, and S. Nagata, "Special articles on LTE-advanced technology: relay technology in LTE-advanced," NTT DOCOMO Technical Journal, vol.12, no.2, pp.29–36, March 2012.
[26] C. Liu, L. Cheng, M. Zhu, and G.K. Chang, "Key microwave-photonics technologies for next-generation cloud-based radio access networks," IEEE J. Lightw. Technol., vol.32, no.20, pp.3452–3460, July 2014.
[27] 3GPP TS 36.213 version 10, "Evolved Universal Terrestrial Radio Access (E-UTRA); Physical layer procedures (Release 10)," June 2011.
[28] R. Tian, T. Ota, and H. Otsuka, "Influence of phase error on OFDM-based 4096-QAM with turbo coding," Proc. ICOIN 2018, F1-5, Jan. 2018.
[29] M. Uezono, S. Nakazawa, S. Matsuoka, and H. Otsuka, "Optimization for time-division relaying against blank subframe ratio and transmission power," Proc. ICUFN 2015, pp.274–276, July 2015.
[30] E. Dahlman, S. Parkvall, and J. Skold, 4G: LTE/LTE-Advanced for Mobile Broadband, Elsevier Ltd., Oxford, UK, 2013.
[31] ITU, "Guidelines for evaluation of radio interface technologies for IMT-Advanced," Report M.2135-1, Dec. 2009.
[32] 3GPP TR 36.814 version 9, "Evolved Universal Terrestrial Radio Access (E-UTRA); Further advancements for E-UTRA physical layer aspects (Release 9)," March 2010.

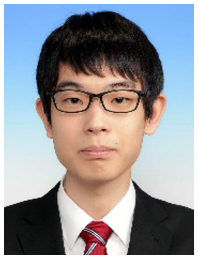

Hiroki Utatsu received the B.S. degree in Information and communication engineering from Kogakuin University, Tokyo, Japan. He is currently working towards the M.S. degree with the Graduated School of Engineering at Kogakuin University. His research interests include mobile communication, heterogeneous networks, and relay networks.

Hiroyuki Otsuka received the B.S., M.S., and Dr. Eng. degrees in electrical engineering from Hokkaido University, Sapporo, Japan, in 1981, 1983, and 1992, respectively. From 1983 to 1999, he was with the Electrical Communication Laboratories, NTT, Yokosuka, Japan, where he worked on digital microwave radio systems and personal handy phone systems, especially in the development of transversal equalizer, interference canceller, and radio on fiber. During the academic year 1990–1991, he was a visiting researcher at the University of Ottawa, Ontario, Canada, where he carried out 256-QAM transmission on fiber. In 1999, he joined NTT DOCOMO, where he worked at Radio Access Development department, and Global Business department. From 2001 to 2003, he was a Vice President of DOCOMO Europe UK, London, UK, where he was involved as W-CDMA technical support. From 2006 to 2010, he was President and CEO of DOCOMO Beijing Communications Laboratories in Beijing, China, where he supported TDD LTE experiments and the standardization for LTE-Advanced. Since 2010, he is a professor of Kogakuin University, Tokyo, Japan. His current research interests include next generation mobile networks, heterogeneous networks, personal cell strategy, fiber-optic relaying, higher-order modulation scheme, and so on. He is a senior member of IEEE.